THERMAL DIFFUSIVITY MEASUREMENTS ON COMPOSITE POROSITY SAMPLES

Joseph N. Zalameda

US Army Aviation Research and Technology
Activity - AVSCOM MS 231
Langley Research Center
Hampton, VA 23665

William P. Winfree

NASA MS231
Langley Research Center
Hampton, VA 23665

INTRODUCTION

Porosity is a defect which can arise from moisture or gases being introduced to the resin system before cure and also during the curing process when poor bagging techniques are used. The effect of porosity results in a degradation in compressive, transverse tensile, and interlaminar shear strengths. For example, for a 1% porosity level there is approximately a 7% decrease in the interlaminar shear strength [1]. Ultrasonics is the current state of the art NDE method for the characterization of porosity in composites using the back scatter and frequency dependent attenuation measurements. In this work a thermal diffusivity technique is investigated for the characterization of porosity in graphite composite parts. The advantages of using thermal techniques is the noncontacting nature of the measurements and the ability to capture large areas using a thermal imager.

In this research the use of a phase lag technique similar to [2], is used to make quantitative measurements of diffusivity in composite porosity samples. The design and calibration of a single point, noncontacting, noncryogenic thermal diffusivity measurement system is described. In addition, the fabrication of 16 ply composite samples with 1, 2, 4, and 8 percent manufactured porosity is presented along with the measurement approach used for maximum sensitivity for defect inspection. Results of the through-ply diffusivity changes due to the varying porosity levels is shown. The relationship between amount of porosity and change in diffusivity is analyzed using an electrical analog for modeling heat flow in the composite.

DIFFUSIVITY MEASUREMENT SYSTEM

The single point diffusivity measurement system used (as shown in figure 1) consists of three main components the heat source, temperature

Review of Progress in Quantitative Nondestructive Evaluation, Vol. 9
Edited by D.O. Thompson and D.E. Chimenti
Plenum Press, New York, 1990

detector, and computer. The heat source consists of a 250 watt infrared heat lamp which is controlled by a TTL clock. The lamp radiation is condensed using a pyrex lens and modulated by a shutter operated by another TTL clock. A PVF2 pyroelectric detector was used to measure changes in IR radiation. Pyroelectric detectors offer good sensitivity, and are rugged, and inexpensive. The infrared detector operates on a change in temperature and since the lamp radiation was modulated no chopping was required. The detector area was 1 mm^2 in size and the measured area was approximately 5 mm^2. The interface electronics contained a high gain preamp connected to a 2 pole low pass Bessel filter. A computer was used to control the modulation of the lamp radiation. The output of the detector and the input to the shutter were digitized at a rate of 256 points per modulation frequency period for four periods. The relative phase of the two signals was calculated from their fast Fourier transforms. Independent measurements were made of the phase contributions of the shutter, PVF2 detector, and associated detector electronics. This was used to reduce the measured relative phase to a phase shift due to the presence of the sample in the system. From this phase shift, and known sample thickness and modulation frequency the diffusivity of the sample was calculated using a one dimension heat flow model for a single layer as discussed later.

SAMPLE PREPARATION

The samples were 16 ply composite plates with a unidirectional lay up of 5208/T-300 prepreg tape. The porosity was fabricated by using hollow carbon spheres varying in diameter from 5-150 microns. The wall thickness of the outer carbon shell was approximately 1-2 microns. The manufacturer's quoted average sphere diameter was 50 microns. The measured size distribution for a given sample of carbospheres is shown in figure 2 and the computed average diameter was 22 microns. This difference may have been due to settling of the larger spheres within the container. Also smaller spheres tended to stick to larger spheres, therefore the number of spheres from the 0-5 microns range may be greater. The spheres were dusted within a defined area 2 inches in diameter between each ply during the lay up procedure. The manufactured porosity levels were 1, 2, 4, and 8 percent by volume. Each sample was approximately 4 by 4 inches in size.

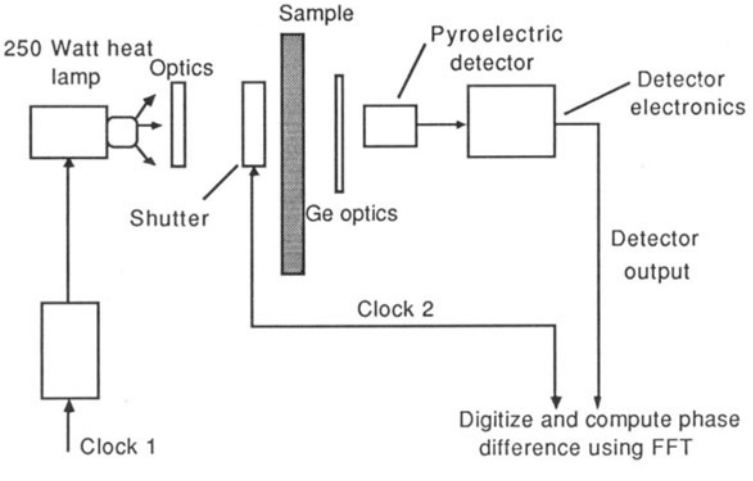

Figure 1. Measurement setup for through ply diffusivity.

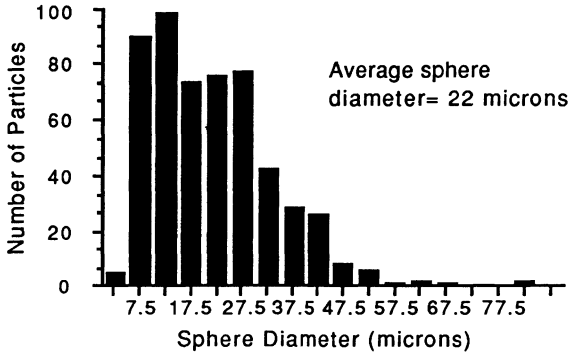

Figure 2. Size distribution of carbospheres.

HEAT FLOW MODEL

The heat flow in a single layer, assuming periodic heating of one surface and no heat flow across the other surface is describe by the equation

$$\frac{\partial^2 T(x)}{\partial x^2} = -\frac{i\omega}{\alpha} T(x) \qquad (1),$$

with boundary conditions:

$$F = K \frac{\partial T(x)}{\partial x} \qquad \text{for } x = 0 \qquad (2),$$

and

$$\frac{\partial T(x)}{\partial x} = 0 \qquad \text{for } x = l \qquad (3)$$

where l is the layer thickness, ω is the angular excitation frequency, α is the thermal diffusivity, T is the temperature and K is the thermal conductivity of the sample. A solution from equations (1-3) can be used to calculate the phase difference between the source modulation and the temperature of the back surface. This phase difference is found to be,

$$\phi = \frac{\pi}{4} + \frac{\sqrt{2}}{2} p l - \tan^{-1}\left(\frac{e^{-\sqrt{2} l p} \sin(\sqrt{2} l p)}{e^{-\sqrt{2} l p} \cos(\sqrt{2} l p) - 1} \right) \qquad (4)$$

where

$$p = \sqrt{\frac{\omega}{\alpha}} \qquad (5).$$

For a multilayered system, the unidirectional heat flow can be represented by an electrical analog. The electrical analog is a series of of low pass

filters each representing a layer [3]. A schematic of the electrical analog of our 16 ply composite is shown in figure 3, with 16 stages corresponding to the 16 plies of the composite. The input heat flux corresponds to the input current I(w) and the temperature at the back face is denoted by the voltage V(w) at node 16. The thermal resistance and capacitance are defined as follows:

$$R = \frac{l_p}{K A} \tag{6}$$

and

$$C = \rho c A l_p \tag{7}$$

where A is area, ρ is density, lp is the ply thickness and c is specific heat. Diffusivity is related to the components of the electrical analogy by

$$\alpha = \frac{lp^2}{R C} \tag{8}.$$

The porosity contribution is estimated by a decrease in conduction area caused by the air filled carbon spheres at the ply interfaces. Each ply of thickness lp and area A is divided into two sub-plys. One containing the voids with thickness lv and the other with thickness lp - lv. Since the voids are spherical in shape the thickness lv is equivalent to the average diameter of the spheres. To model the sub-ply with voids an interface resistance is added to the voidless electrical model as shown in figure 4. The interface resistance is a parallel combination of the resistances due to the area occupied by the spherical voids and the area remaining in contact. In a parallel combination the total value of the resistance is never greater than the smallest value. As the amount of porosity increases, its contribution to the resistance decreases with more heat flow through the porous region. The resistance equations are shown as follows:

$$R_{por} = \frac{l_v}{K_p A_{por}} \tag{9}$$

and

$$R_{cont} = \frac{l_v}{K (A - A_{por})} \tag{10}$$

where lv is the average diameter of the voids, Kp is the thermal conductivity of the voids, and Apor is the area occupied by the spherical voids. The void areas were calculated using the known normalized volume porosity contents and the measured average diameter. The thermal conductivity of the spherical voids are due to the outer carbon shell and conduction within the air gap. Diffusivity is related to the electrical components of this electrical analog by

$$\alpha = \frac{l_p^2}{(R + \frac{R_{por} R_{cont}}{R_{por} + R_{cont}}) C} \tag{11}.$$

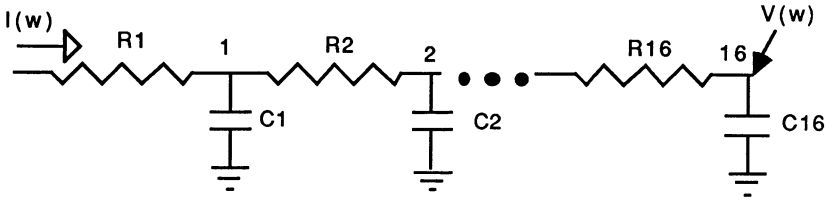

Figure 3. Electrical model of unidirectional heat flow.

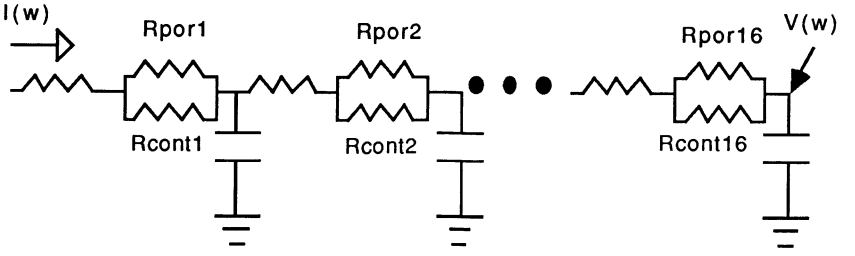

Figure 4. One dimensional thermal model with porosity.

MEASUREMENT APPROACH

The magnitude of the measured temperature oscillation decreases by

$$e^{-x\sqrt{\frac{\omega}{2\alpha}}} \qquad (12)$$

as the thermal wave propagates [4]. Typically $(2\ \alpha/\omega)^{1/2}$ is defined as the "thermal diffusion length" in the material of interest and experimentally this length is kept on the order of the thickness of the sample. For our composite samples with typical through ply diffusivities of .0043 cm^2/sec and thicknesses of .254 cm, this requires the frequency be on the order of .02 Hz and frequencies in this range were used. Figure 5 shows the signal attenuation as a function of heating frequency for a 16 ply composite plate. It is desired that the correct heating frequency is used for maximum sensitivity to changes in diffusivity. The derivatives of equation (4) with respect to diffusivity and thickness are plotted using typical values of .0043 cm^2/sec for diffusivity and .254 cm for thickness. The result in figure 6 show at higher heating frequencies the change in phase with respect to a change in diffusivity increases in magnitude. Likewise in figure 7 the change in phase with respect to a change in thickness also increases as the frequency is increased. Analysis reveals the measurement is slightly more sensitive to changes in thickness than to changes in diffusivity. To discriminate the phase changes it is important to know the thickness. With the sample thickness known, higher frequencies give more sensitivity to diffusivity, however as shown in figure 5 the measured temperature response decreases thereby establishing the bandwidth. After considering all factors .35 hertz was selected as the optimum modulation frequency.

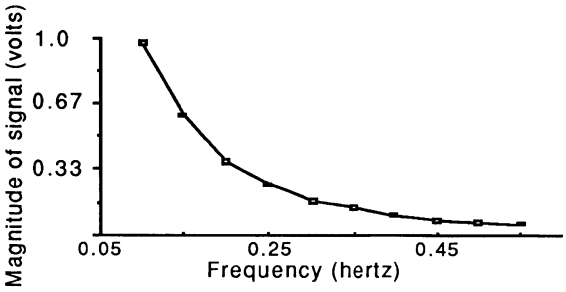

Figure 5. Measured attenuation of signal.

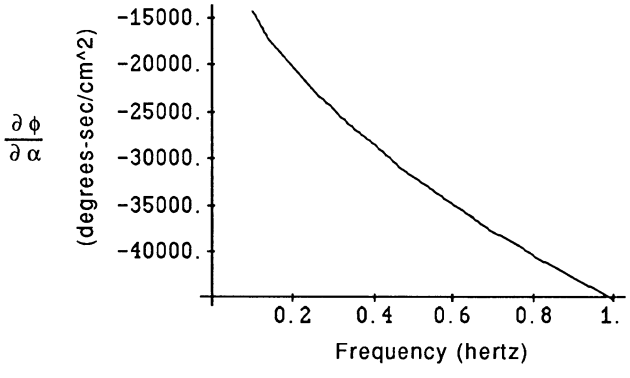

Figure 6. Sensitivity to diffusivity.

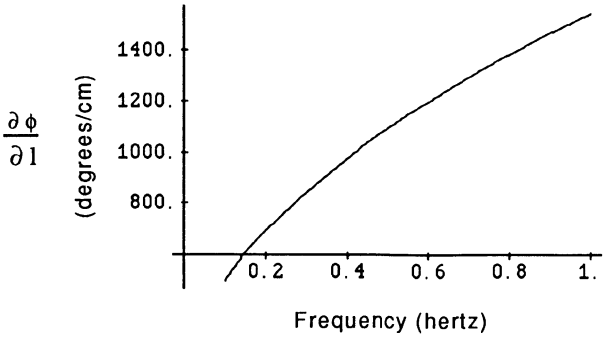

Figure 7. Sensitivity to thickness.

RESULTS

A plot of the measured phase with respect to frequency for each of the porosity levels is shown in figure 8. Each point represents an average of five measurements. From figure 8 the difference in phase between samples of different porosities increases as the frequency increases as expected from figure 6. For each frequency the diffusivity can be calculated using equation (4). A slight unexpected variation in calculated diffusivity with frequency was found for these samples. This is suspected to be a result of lateral heat flow in the samples. For the purpose of comparison the diffusivity from measurements at .35 hertz was used. The change in diffusivity as a function of porosity is shown in figure 9. Also shown in figure 9 is the results of the electrical analog model for the different porosities. As can be seen from the figure the agreement between the model and measurements is very good. The average diameter of the spheres (or thickness of sub ply with porosity) used in the model was 27 microns. This value was slightly higher than the histogram average diameter of 22 microns. This slightly larger value may have been due to the clumping effects of the smaller spheres 5 microns and less. The carbon spheres thermal conductivity value used in the model was .0025 W/C-cm slightly more than the manufacture's quoted value of .0017.

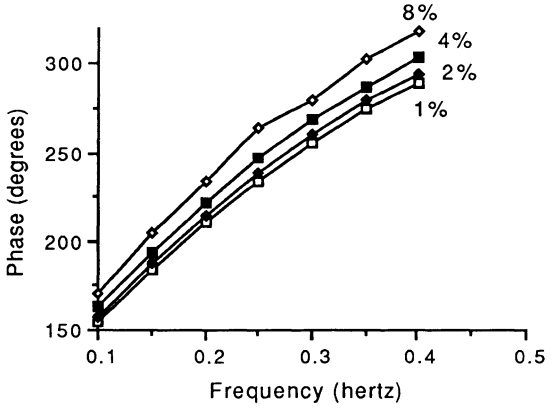

Figure 8. Measured phase response.

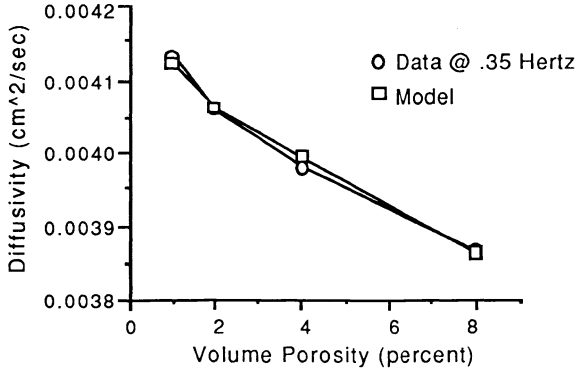

Figure 9. Comparison of measured diffusivity to the model.

The thermal conductivity of the fiber/matrix value used in the model was .0132 W/C-cm. This value is contingent on the fiber volume fraction ratio.

CONCLUSIONS

Characterization of simulated porosity in graphite composites can be accomplished by thermal diffusivity measurements. Since the porosity was simulated using hollow carbon spheres it is expected that "real world" porosity would produce greater diffusivity changes due to a lower thermal conductivity. It has been demonstrated that it is possible to model this change in diffusivity with a simple electrical analog and an assumption that the porosity changes the contact resistance between plies. The measurement uncertainty was calculated to be no more than 2 percent for an average of five diffusivity measurements.

Future work will require destructive tests to find the fiber volume fraction ratios for verification of the thermal conductivity value used in the model. Also the use of a thermal imaging system in conjunction with a real time image processor for diffusivity mapping over large areas will be an improvement over the single point detector system used. Finally the need for inspection of actual industrial porosity samples in conjunction with ultrasound would be appropriate.

ACKNOWLEDGEMENTS

The authors would like to thank Anton Schuzler II and Ravi Shenoy for their work in obtaining the size distribution of the carbospheres. Also Robert Edahl for quick work in obtaining sample photomicrographs.

REFERENCES

1. N. Judd, W. Wright, SAMPE Journal January/February, pp. 10 -14 (1978).

2. A. Hirschman, J. Dennis, W. Derksen, T. Monahan, International Developments in Heat Transfer, ASME, Part IV, pp. 863-869.

3. F. Incropera, P. Dewitt, Fundamentals of Heat Transfer (John Wiley and Sons, Inc., 1981).

4. H. Carslaw, J Jeager, Conduction of Heat in Solids, (Oxford University Press, 1959).